No.22- (3) 2019 Journal of Petroleum Research & Studies (JPR&S)

Thermal Analysis of In-Service Welding Process for Pipeline

Dr.Karima E. Amori[*], Mohamed N. Hussain[**] and Hadeel B. Hilal[*]

[*]Univ. of Baghdad/ Mech. Eng. Dept., [**]Petroleum Research & Development Center

Corresponding Author E-mail: hadeelmechano@yahoo.com

Abstract

A numerical model had been developed using three dimensional finite element method to predict temperature history of pipe wall thickness by using a FORTRAN computer program. The developed numerical model concerned with the effect of power and velocity of moving heat source, temperature dependent material properties, and transient heat transfer and phase change transformation. Also the effect of heat flux and flow rate on cooling time was investigated numerically.

An experimental setup had been designed, manufactured and instrumented to investigate the thermal history of an in-service welding process considering air as the flowing fluid inside test pipe. The burn-through was investigated experimentally under the influence of gas flow rate, heat flux and the depth of defect presented in pipeline wall. It has been concluded that the burn-through do not occur for the studied parameter range. The results showed that as the flow rate increases from (24 - 30 lpm) the cooling time decrease by a rate of (11.7 %) and when the flow rate increase from (24-60 lpm) the cooling time decrease by a rate of (41.1 %) without affecting peak temperature with pipe wall thickness of (6mm). Also it has been concluded that as the heat flux increases from (1110- 1370 kJ/mm) the peak temperature increases with a rate of (22.11 %) and cooling time increase with (25.4 %) when the heat flux increases from (1110- 1659 kJ/mm) the peak temperature increases with a rate of (46.86%) and cooling time increase with (50.7 %) with pipe thickness of (6mm).

Keywords: In-Service Welding, Temperature History, moving heat source, burn-through, numerical modeling.

التحليل الحراري لعملية اللحام أثناء الخدمة للأنابيب

الخلاصة

تم بناء نموذج عددي باستخدام طريقة العناصر المحددة ثلاثية الأبعاد للتنبؤ بقيم درجات الحرارة مع الزمن على جدار الأنبوب باستخدام برنامج FORTRAN وكان بناء النموذج العددي يعتمد على مصدر حراري متحرك، مادة متغيرة المواصفات مع درجات الحرارة وانتقال حرارة غير مستقر لمادة متغيرة الطور. كذلك تم دراسة تأثير كل من الحرارة المسلطة ومعدل جريان المائع داخل الأنبوب على معدل التبريد لمنطقة اللحام. تم تصميم وتصنيع وتجهيز متحسسات قياس لدراسة التوزيع الحراري لعملية اللحام أثناء الخدمة حيث اعتبر الهواء هو المائع الذي يجري داخل الأنبوب. ظاهرة الاحتراق خلال الجدار فحصت مختبريا تحت تأثير كل من معدل جريان الهواء، الحرارة المسلطة وعمق العيب الموجود على جدار الأنبوب وقد استنتج إن الظاهرة لا تحدث لنطاق العناصر المدروسة. أظهرت النتائج أن زيادة معدل الجريان من (24 - 30 lpm) تؤدي إلى نقصان معدل تبريد منطقة اللحام بنسبة (11.7 %) وزيادته من (24-60 lpm) تؤدي إلى نقصان وقت تبريد منطقة اللحام بنسبة (41.1 %) دون التأثير على قيمة درجة الحرارة القصوى لسمك جدار أنبوب (6mm). كذلك أظهرت النتائج أن زيادة الحرارة المسلطة من (1110- 1370 kJ/mm) تؤدي إلى زيادة درجة الحرارة القصوى بنسبة (22.11 %) و زيادة وقت التبريد بنسبة (25.4 %) وزيادتها من (1110- 1659 kJ/mm) تؤدي إلى زيادة درجة الحرارة القصوى بنسبة (46.86%) و زيادة وقت التبريد بنسبة (50.7 %) لسمك جدار أنبوب (6mm).

الكلمات الرئيسية: لحام أثناء الخدمة، التاريخ الحراري، مصدر حراري متحرك، الاحتراق خلال الجدار، نموذج عددي.

Introduction

In long-distance pipelines, defects can occur as a result of construction faults, corrosion, third party interference, and ground movement [1]. When a segment of pipeline is found to be corroded or local damaged, one of the conventional repair methods is that the sections of the pipeline would have to be sealed and degassed before any welding process and then purged before reinstatement. However, the cost is high in terms of venting and stopping the interior media supply. In addition, some of interior fluid leaks into the atmosphere which are wasteful and also environmentally damaging actions [2, 3]. Welding onto a pipeline in active operation called in-service welding, it is an advance technique employed to repair, modify or extend of pipelines. These methods are widely used in guaranteeing the safe transmission of petroleum and natural gas. There are two concerns

during in-service welding the first one is the possibility of burn-through during the welding process which is due to the localized heating, leading to the loss of material strength on the inner surface of the main pipe. The pipe wall may burst under internal pressure if the loss of the strength is significant. The second concern is the high cooling rate of the weldment or quick removal of heat from the pipe wall as a result of forced convection due to the fluid flow through the main pipe. The high cooling rate can promote the formation of heat affecting zone (HAZ) microstructure with high hardness making the weldment susceptible to cracking therefore, by implementing proper heat input and appropriate in-service welding procedure optimal (HAZ) hardness can be obtained with low risk of burn-through. In 1999, Oddy and Mcdill [4] have tried to provide guidelines in predicting burn-through by comparing the results of a three dimensional thermo-mechanical finite element by analysis of welding on pressurized vessels with experimental data. It has been observed that burn-through does not occur as long as temperature at inside surface does not exceed 980˚C. In 2005, Wahab et al. [5] have developed a new approach to the problem of burn-through based on the thermo-elastic plastic models and they have directly simulated the pipe bursting during welding. In 2002, Cisilino et al. [6] evaluated numerically the minimum weldable thickness needed on the pipe for avoiding burn-through during girth welding of the reinforcement to the pipe. They concluded that when the pressure is (100% OP) minimum weldable thickness was (4.65mm) and for gas pressure equal to (80% and 60% OP) minimum weldable thickness is (4.8 and 5.3 mm) respectively. They also concluded that the minimum thickness increase when the gas flow increases.

In the present work a thermal experimental and numerical study is accomplished on welding process of pipeline to study the influence of air inside the pipe on temperature history. Also the burn-through was investigated under the influence of air flow rate, arc heat flux and defect depth.

Mathematical Model:

1. Governing Equation:

The general equation of conduction heat transfer for an isotropic material is used to describe the pipe wall thermal history [7].

$$\frac{\partial^2 T}{\partial x^2}+\frac{\partial^2 T}{\partial y^2}+\frac{\partial^2 T}{\partial z^2}+\frac{\dot{q}}{k}=\frac{1}{\alpha}\frac{\partial T}{\partial t} \quad (1)$$

where $\dot{q}$ is the heat generation per unit volume, k is the thermal conductivity of the test pipe material, α is the thermal diffusivity of metal at time t.

$$\dot{q}=\rho H\frac{\partial f_s}{\partial t} \quad (2)$$

H is the latent heat of fusion of the metal (due to phase change), ρ is the density.

2. Initial and Boundary Conditions:

The pipe metal initial temperature is assumed uniform and equal to $T_\circ$, i.e.

$$T_{(x,y,z)}=T_\circ \quad (3)$$

The convection boundary condition on the upper surface of the welded pipe (which in contact with ambient air) can be formulated using Newton's law of cooling, which is

$$q_{conv\ upper}=h_{upper}A\,(T_w-T_\infty) \quad (4)$$

Where T_w is the pipe transient unknown temperature ˚C, T_∞ is the ambient temperature ˚C.

The pipe ends will considered as an insulated faces no heat flow crosses these boundaries, which lead to :-

$$k\frac{\partial T}{\partial x_i}=0 \quad (5)$$

Where i refer to x or z coordinate

The convection boundary condition on the lower surface of the welded pipe (which is in contact with the flowing air) can be formulated using Newton's low of cooling, which is

$$q_{conv\ lower}=h_{lower}A\,(T_w-T_a) \quad (6)$$

Where T_a is the air temperature.

3. Convective Heat Transfer Coefficients:

Simplified equation for the convective coefficient of heat transfer from the upper surface of welded pipe exposed to air at T_∞ is given by [8] based on natural convection by:-

$$h_{upper} = 0.59 \left(\frac{\Delta T}{L}\right)^{\frac{1}{4}} \quad (7)$$

Where h_{upper} is the heat transfer coefficient, W/m^2.˚C, ΔT is the temperature difference between pipe wall (T_w) and ambient temperature T_∞,˚C, such that

$\Delta T = T_w - T_\infty$

L is the surface length that exposed to air, m

The bottom surface is affected by forced convection (flow of air). Its heat transfer coefficient is calculated by the following equations [**9, 10]:**

$$pr = \frac{\mu_a . c_{pa}}{k_a} \quad (8)$$

$$Re = \frac{V_a . d}{\nu_a} \quad (9)$$

$$Nu = 0.023 \times Re^{0.8} \times Pr^{0.4} \quad (10)$$

$$h_{lower} = \frac{k_a . Nu}{d} \quad (11)$$

where Pr denotes Prandtl number, μ_a is the dynamic viscosity, c_{pa} the specific heat, k_a thermal conductivity, Re Reynolds number, V_a is the mean velocity of the fluid, d is the tube diameter, ν_a is the kinematic viscosity, Nu denotes the Nusselt number.

4. Solidification Equilibrium :

For equilibrium solidification, the solid fraction f_s is related to the temperature such that

$$f_s = \frac{1}{1-k_\circ} \left(\frac{T-T_L}{T-T_f}\right) \quad (12)$$

where T_L is the liquids temperature and T_f is the freezing temperature of the pure material of the pipe wall. The second case leads to Scheild equation relating the fraction to temperature.[11]

$$f_s = 1 - \left[\frac{T_f - T}{T_f - T_l}\right]^{\frac{1}{(k_\circ - 1)}} \quad (13)$$

For linear relationship the value of $1/(k_\circ - 1)$ is equal to 1, and equation can be written

as:-

$$f_l = [\frac{T_f - T}{T_f - T_l}] \quad (14)$$

Numerical Analysis

1. Finite Element Method (FEM) Formulation:

The unknown temperature T is approximated in the elemental solution domain at any time by:

$$T = \sum_{i=1}^{p} N_i \, T_i(t) \quad (15)$$

T_i Is the instantaneous temperature value of node I, and p is the number of elemental nodes, and N_i is a linear interpolation functions. Discretizition of equation (1) is adopted with FEM to give elemental matrices and vector. The assembly of these elemental matrices into global matrices and vector give first order transient simultaneous differential equations of the form [7,12]:

$$[k_3]\dot{\vec{T}} + [k]\vec{T} = \vec{P} \quad (16)$$

$$[k_3] = \sum_{e=1}^{E} [k_3^{(e)}] \quad (17)$$

$$[k] = \sum_{e=1}^{E} \left[\left[k_1^{(e)} \right] + \left[k_2^{(e)} \right] \right] \quad (18)$$

and

$$\vec{P} = \sum_{e=1}^{E} \vec{P}^{(e)} \quad (19)$$

$$k_{1_{ij}}^{(e)} = \iiint_{v^{(e)}} \left(k_x \frac{\partial N_i}{\partial x} \frac{\partial N_j}{\partial x} + k_y \frac{\partial N_i}{\partial y} \frac{\partial N_j}{\partial y} + k_z \frac{\partial N_i}{\partial z} \frac{\partial N_j}{\partial z} \right) dv \quad (20)$$

$$k_{2_{ij}}^{(e)} = \iint_{k_3^{(e)}} h \, N_i N_j \, ds_3 \quad (21)$$

$$k_{3_{ij}}^{(e)} = \iiint_{v^{(e)}} \rho c N_i N_j \, dv \quad (22)$$

and

$$\vec{P}^{(e)} = \iiint_{v^{(e)}} \dot{q} N_i \, dv - \iint_{s_2^{(e)}} q N_i ds_2 + \iint_{s_3^{(e)}} h T_\infty N_i ds_3 \quad (23)$$

2. Grid Generation:

The physical domain is divided into sub divisions (1920) and (3069) nodes including the work piece and the backup metal. Fig.1. shows subdivision of the volume.

3. Transient Solution by θ -Method :

The procedure relies on diving recursion formulas relate the values of {T} at one instant of time t to the values of {T} at a later time $t + \Delta t$, where Δt is the time step. The recursion formulas make it possible for the solution to be "marched" in line, starting from the initial conditions at time t=0 and continuing step by step until reaching the desired duration. Let in denote a typical time in the response so that [**12**].

$$t^n = t^\circ + \Delta t \qquad (24)$$

where superscripts (n,0) refer to new and old respectively.

A general family algorithms result by introducing a parameter θ such that:-

$$[K_3]\{\dot{T}\}_\theta + [K]\{T\}_\theta = \{P\}_\theta \qquad (25)$$

where $0 \leq \theta \geq 1$

Introducing the approximations:

$$\{\dot{T}\}_\theta = \frac{\{T\}^n - \{T\}^\circ}{\Delta t} \qquad (26)$$

$$\{T\}_\theta = (1-\theta)\{T\}^\circ + \theta\{T\}^n \qquad (27)$$

$$\{P\}_\theta = (1-\theta)\{P\}^\circ + \theta\{P\}^n \qquad (28)$$

Substituting equation (27) and (28) into equation (26) yields:

$$\left[\theta[K] + \frac{1}{\Delta t}[K_3]\right]\{T\}^n = \left[-(1-\theta)[k] + \frac{1}{\Delta t}[K_3]\right]\{T\}^\circ + (1-\theta)\{P\}^\circ + \theta\{P\}^n \qquad (29)$$

here the vector $\{T\}^n$ on this L.H.S of this equation are unknowns, and all of the terms on the R.H.S are known. Equation (29) represents a general family of recurrence relation. The value of θ is taken as (2/3) by adopting Galerlcin method to ensure stable and converged solution. Equation (29) becomes [**12**]:

$$\left[\frac{2}{3}[K] + \frac{1}{\Delta t}[K_3]\right]\{T\}^n = \left[\frac{-1}{3}[K] + \frac{1}{\Delta t}[K_3]\right]\{T\}^\circ + \frac{1}{3}\{P\}^\circ + \frac{2}{3}\{P^n\} \qquad (30)$$

This equation can be rewritten in matrix form:

$$AX = B \qquad (31)$$

Where:

$$A = \left[\frac{2}{3}[K] + \frac{1}{\Delta t}[K_3]\right]$$

$$X = \{T\}^n$$

$$B = \left[\frac{-1}{3}[K] + \frac{1}{\Delta t}[K_3]\right]\{T\}^\circ + \frac{1}{3}\{P\}^\circ + \frac{2}{3}\{P^n\}$$

4. Computational Procedure:-

A Fortran computer program is developed to solve the temperature distribution within the pipe wall. The computer program includes the following subroutines:

1. Input data (welding current, speed and voltage), thermo physical properties of welded metal, initial temperature, environmental temperature, thickness and length of the welded pipe.
2. Generating the mesh nodes, elements and defining the topology matrix to link the global nodes number with the local number and calculating the elemental area.
3. calculation and assembly of transient elemental :
   a) Conduction matrix $\left[k_1^{(e)}\right]$.
   b) Capacitance matrix $\left[k_3^{(e)}\right]$
   c) Convection matrix $\left[k_2^{(e)}\right]$.
   d) Heat generation vector $\vec{P}_1^{(e)}$
   e) Heat source vector $\vec{P}_2^{(e)}$
   f) Convection vector $\vec{P}_3^{(e)}$.
4. Solve equation (29) by Gauss elimination method for symmetry matrix for new nodal temperature profile.
5. Increase time by Δt then repeat steps 3, and 4.

The general computer program flow chart is shown in Figure (2).

Experimental Apparatus and Procedure

1. Experimental setup:

The experimental rig consists of compressor, test section and cooling system. A compressor type Balma 150 compressor which is compress to (10 bar) as maximum is used to supply air to the rig.

The Test section was a low carbon steel pipe with (101.6mm) inside diameter, (6mm) wall thickness and (1800 mm) in length. The pipe receives air from the compressor and discharges it to the environment. A defect is machined in the test section and then it is welded in order to make the experimental tests. A Cooling System was also used in the experimental rig which is consists of three parts the first one is the Cooling coil which is made of copper pipe of diameter (9.525mm). It designed according to the equation:

$$L = N\sqrt{(2\pi r)^2 + P^2} \quad (1)$$

Where L denotes coil length, N is the number of turns, r is the coil radius, and P is the pitch. It is used to cool the main pipe to decrease the temperature of the air so it will cool the molten pool during the process of welding. The second part is the Pump which is used for pumping the water through the cooling coil from the tank. The head of the pump is (9-12 m). The operating voltage required is (220 V) and the current is (2.5 Amp). The third part is galvanized water storage of dimension (500 * 500 *500 mm^3) with a thickness of (1.8mm) is used to feed water to the pump. The BX1 series AC arc welding machine was used in the welding process which is a kind of AC arc welding power supply.

Thermocouples type (k) is used to measure the temperatures at selected points. Type (k) thermocouple consists of chromel -alumel with a sensitivity of (41μv/C˚) and temperature range of (-200C˚ to +1350 C˚). The thermocouples connected to the data logger which records the temperatures varying with time and save them in an SD card in the form of excel sheet. The data logger used consists of 12 channels temperature recorder. The pressure transducer type DRUCK LTD S/N 18770 of (0 to 5000 mbar) range with pressure indicator is used in order to show the pressure value. Two pressure transducer were used to measure the inlet and outlet pressure of test pipe. A flow meter with a reader is used in order to measure the rate of air or gas flowing through the test pipe which is

installed at the test pipe inlet. The flow meter and reader used is S-meter TFB-100 which is designed for LPG in liquid phase. The flow rate rang is (0.04-0.25 m^3/h of liquid LPG) with measurement accuracy of (± 0.5%). Figure (3) Shows experimental rig.

2. Experimental Work

An experimental rig was designed, manufactured and instrumented in order to make the experimental tests which is representing by an in-service welding process for a non-through holes of (4mm) in diameter machined by a manual drilling with different depths and welding them by supplying different values of heat flux and different air flow rates to study the influence of these parameters on the burn-through.

Results and Discussion

- **Experimental Results:**

  Welding a non-through holes (dead end holes) of (4mm) in diameter with different depths (2, 3 and 4mm) and apply different current (64, 79, and 94 Ampere) with different air flow rate (24, 30 and 60 lpm). These tests were carried out in order to study the burn-through possibility which is affect by three parameters which are internal pressure, heat input by welding arc and thickness of the wall or depth of defect. Thermocouples are fixed around the hole as shown in Figure (4). Table (1) shows the results for in-service welding process of non-through holes when air is considered as the flowing fluid inside the test pipe for 27 tests. The table shows maximum temperature, period of maximum temperature and cooling time after welding process needed to reach a temperature of approximately (250˚C) for each test. The results showed that as the air flow rate increase the cooling time decrease. Figure (5) shows the symmetry in the experimental temperature history between the right and left nodes from the hole for experiment (No.19) in which the hole depth, current and voltage applied were (4mm, 64 Ampere and 56.4 Volt) with air flow rate equal to (24 lpm). Figure (5b) explain that maximum temperature is approximately (700˚C) belong to

node 2 and (610 ˚C) for node 2'. It has been concluded that there is no risk of burn-through for the studied parameters range.

- **Computational Results:**

The welding current, voltage, electrode movement speed and thermodynamic properties of the test pipe material are fed to the computer program to investigate the temperature history for the welding region for one test of the experimental work. This numerical test represents an in-service welding process for a dead end hole (test No.19). The welding heat flux is to be uniform and applied on the hole area also the wave technique of the electrode movement is neglected in the computational solution. Figure (6a) shows the computed temperature history for nodes (2, 2', 4, and 4'). The maximum temperature is approximately (530˚C) while Figure (6b) indicates temperature history for nodes (1, 1', 5, and 5'). The maximum temperature for it was approximately (610 ˚C). The computational results explain that the temperature history is symmetry between nodes (1, 1', 5, and 5') likewise that for nodes (2, 2', 4, and 4'). Figure (7) shows computational temperature distribution along z axis at (x=17.224 mm) for (experiment No. 19). Figure (7a) shows temperature distribution at (t=6s of the welding process) in which the maximum temperature is approximately (730 ˚C). Figure (7b) illustrate temperature distribution at (t=36s of the welding process) in which the maximum temperature is approximately (475 ˚C). Figure (7c and d) explain temperature distribution at (t=50s and t=70s of the welding process respectively) in which the maximum temperatures are approximately (375 ˚C and 290 ˚C). Figure (8a) explains the effect of flow rate variation on temperature history at constant heat flux of (1110 kJ/mm). The figure explain that as the flow rate increases from (24-30 lpm) the cooling time decrease by a rate of (11.7 %) and when the flow rate increase from (24-60 lpm) the cooling time decrease by a rate of (41.1 %) without affecting peak temperature. Figure (8b) explains the effect of heat flux variation on temperature history at constant flow rate of (24 lpm). The figure explain that as the heat flux increases from (1110-1370 kJ/mm) the peak temperature increases with a rate of (22.11 %) and cooling time increase with (25.4 %) when the heat flux increases from (1110- 1659 kJ/mm) the peak

temperature increases with a rate of (46.86%) and cooling time increase with (50.7 %).

- **Comparison between Experimental and Computational Results:** Figure (9a) shows a comparison between computational and experimental temperature history for nodes (1 and 1'). The figure shows that the computed maximum temperature is slightly below the experimental maximum temperature for node (1'), and slightly above the experimental maximum temperature for node (1). Figure (9b) shows a comparison between computational and experimental temperature history for nodes (2 and 2'). The figure shows that the computed maximum temperature is lower than the experimental maximum temperature with a difference approximately equal to (180 and 90 ˚C) from nodes (2 and2') respectively. Figure (9c) shows a comparison between computational and experimental temperature history for nodes (4 and 4'). The figure shows a good agreement between the computed maximum temperature and the experimental maximum temperature for node (4'), while that for node (4) there is a difference approximately (280 ˚C) between the computational and experimental maximum temperature. Figure (9d) shows a good agreement between computational and experimental temperature history for nodes (5 and 5') in maximum temperature. The observed difference in the computational and experimental maximum temperature for Figures (9a), (9b), and (9c) is due to the assumption of uniform welding heat source that considered in the computational work in other hand there was no consideration of wave technique for the welding electrode movement of experimental work in the theoretical analysis. There was a good agreement in the heating time. The difference in cooling time was related to the neglecting of radiation effect in the computational analysis.

Conclusions

A 3D FE model was developed to simulate in-service welding process. The model was used to predict temperature history of pipe wall. Good agreement was obtained with local thermocouples locations. During in-service welding, the flowing air will take away

mach of the heat, which accelerate cooling rate of the welding zone. It was concluded that burn-through do not occur for the ranged parameter studied under the influence of internal pressure, heat flux and defect depth variation. The results showed that as the flow rate increases from (24 - 30 lpm) the cooling time decrease by a rate of (11.7 %) and when the flow rate increase from (24-60 lpm) the cooling time decrease by a rate of (41.1 %) without affecting peak temperature when the pipe thickness is (6mm). Also it has been showed that as the heat flux increases from (1110- 1370 kJ/mm) the peak temperature increases with a rate of (22.11 %) and cooling time increase with (25.4 %) when the heat flux increases from (1110- 1659 kJ/mm) the peak temperature increases with a rate of (46.86%) and cooling time increase with (50.7 %) when the pipe thickness is (6mm).

Table (1) Results of the In-Service Welding process for Non-Through Holes

t=4mm	24 lpm				30 lpm				60 lpm			
current Ampere	No.	T max (˚C)	T max period (s)	Cooling time (s)	No.	T max (˚C)	T max period (s)	Cooling time (s)	No.	T max (˚C)	T max period (s)	Cooling time (s)
64	1	1292	2	16	4	1301	3	12	7	943.8	2	10
79	2	1115	2	14	5	1058	2	11	8	961.4	3	9
94	3	980.1	3	11	6	1266	2	13	9	1236	3	10

t=3mm	24 lpm				30 lpm				60 lpm			
current Ampere	No.	T max (˚C)	T max period (s)	Cooling time (s)	No.	T max (˚C)	T max period (s)	Cooling time (s)	No.	T max (˚C)	T max period (s)	Cooling time (s)
64	10	923	2	10	13	1126	2	9	16	1224	2	7
79	11	922.1	3	8	14	1032	3	6	17	915.7	2	6
94	12	1356	2	14	15	1351	2	11	18	933.3	2	7

t=2mm	24 lpm				30 lpm				60 lpm			
current Ampere	No.	T max (˚C)	T max period (s)	Cooling time (s)	No.	T max (˚C)	T max period (s)	Cooling time (s)	No.	T max (˚C)	T max period (s)	Cooling time (s)
64	19	819.2	3	7	22	649.3	3	4	25	1028	2	7
79	20	1228	2	10	23	802.1	2	6	26	1038	2	7
94	21	1241	2	11	24	946.8	2	7	27	906.7	3	5

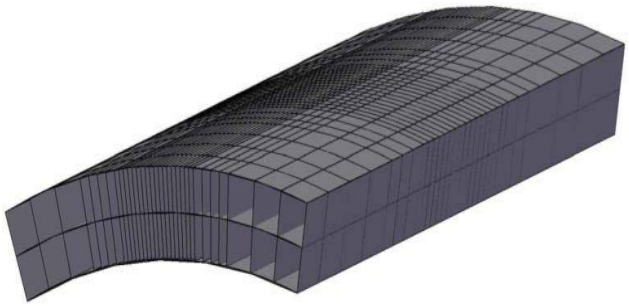

Fig. (1) Grid generation

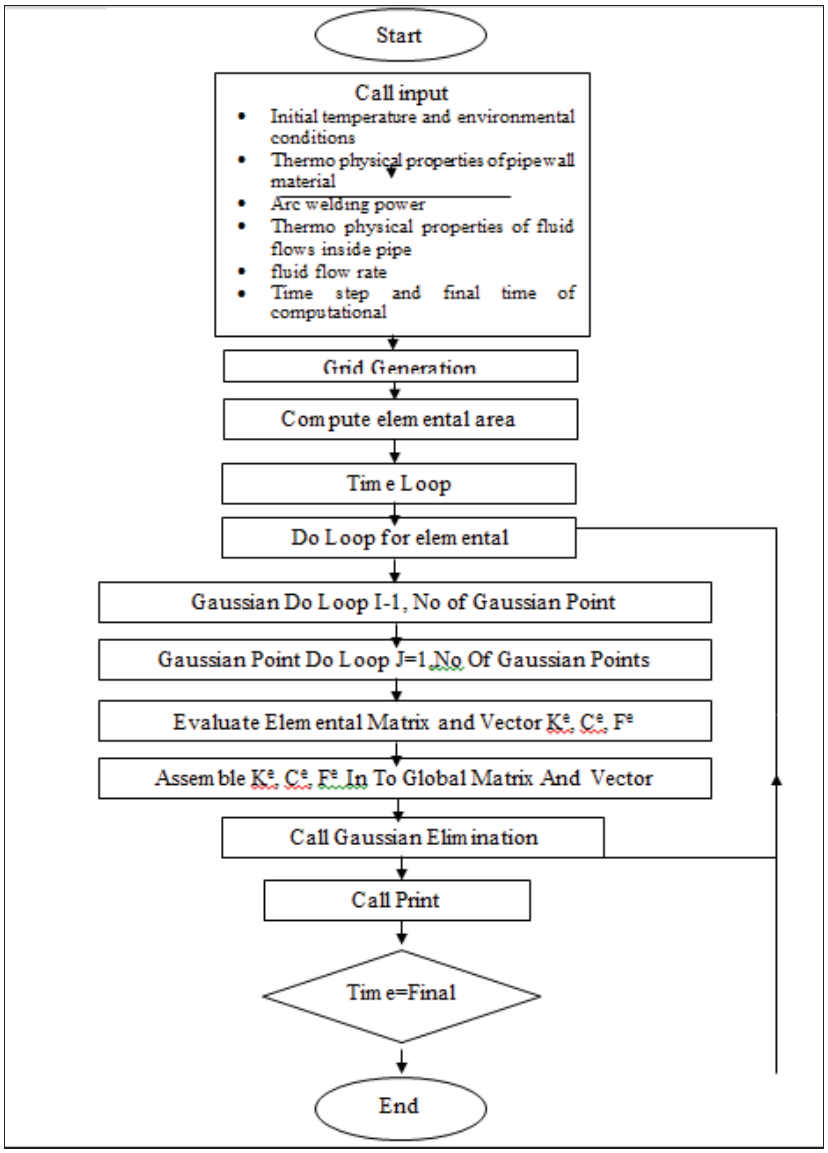

Fig. (2) The General Computer Program Flow Chart

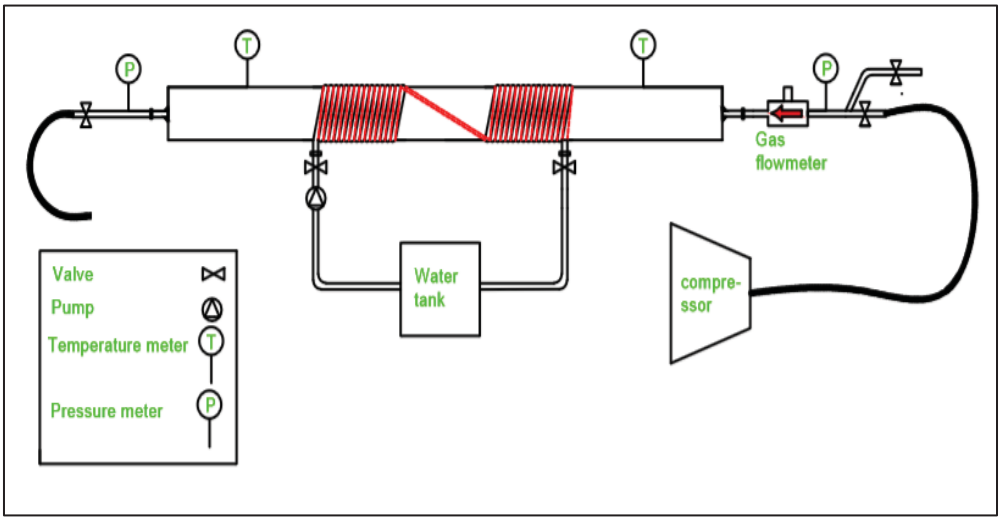

Fig. (3) Experimental setup

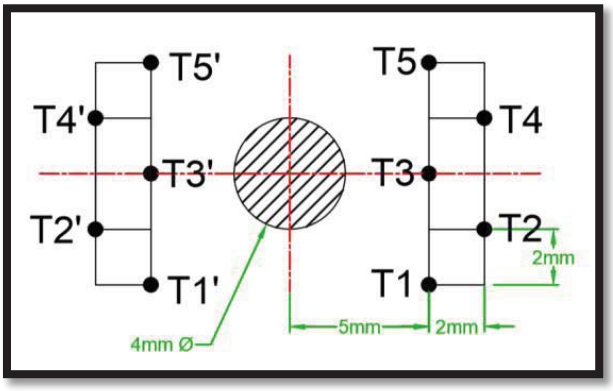

Fig. (4) Thermocouples Positions around the Dead End Hole

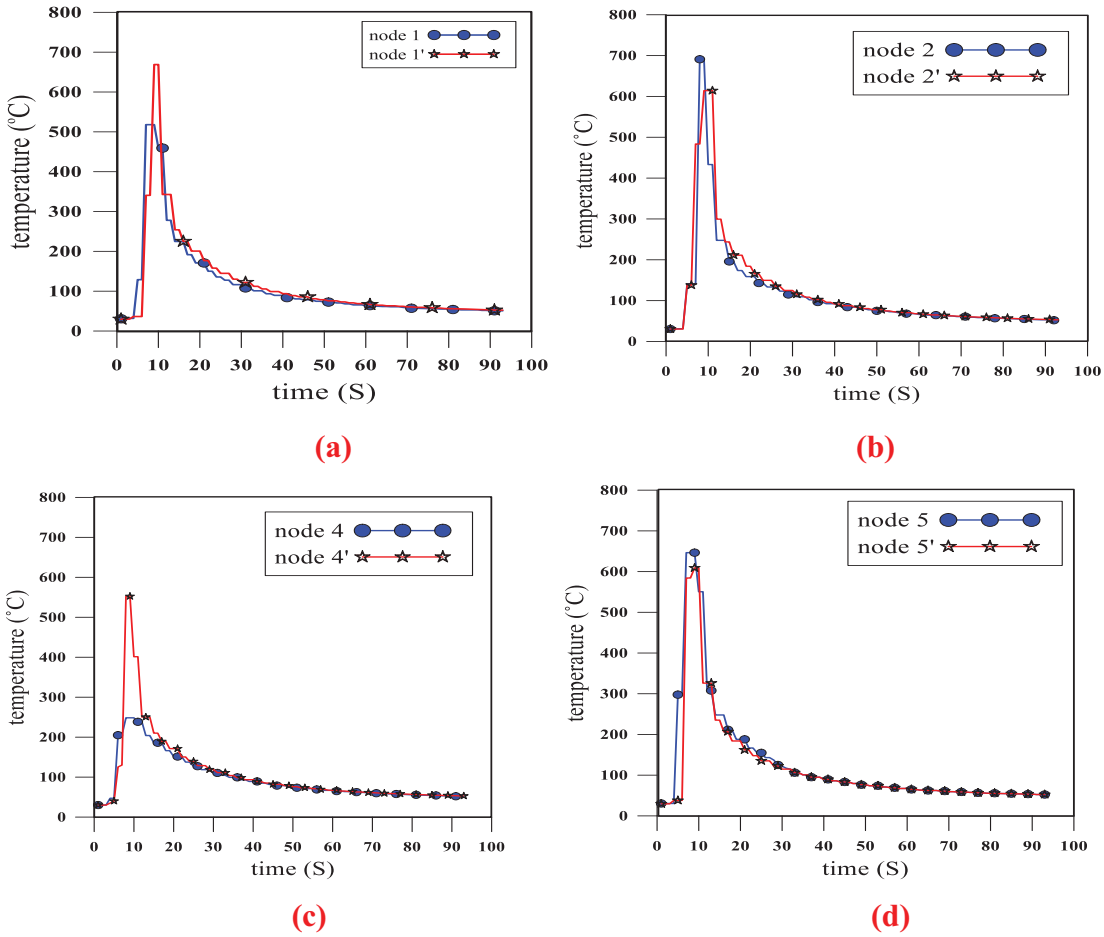

Fig. (5) Experimental Temperature History for Experiment (19) , a) 1 and 1', b) 2 and 2', c) 4 and 4', d) 5 and 5'

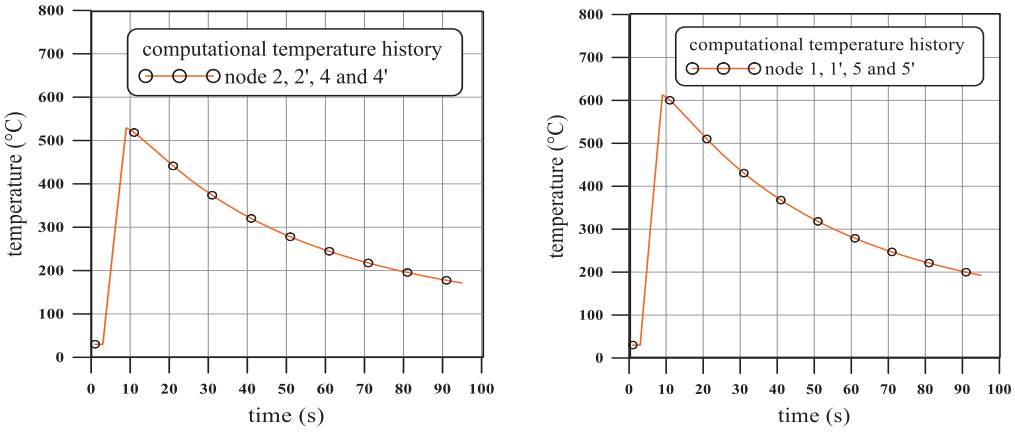

Fig. (6) Computational Temperature History for Experiment (No.19), a) 2, 2',4 and 4' b) 1, 1', 5 and 5'

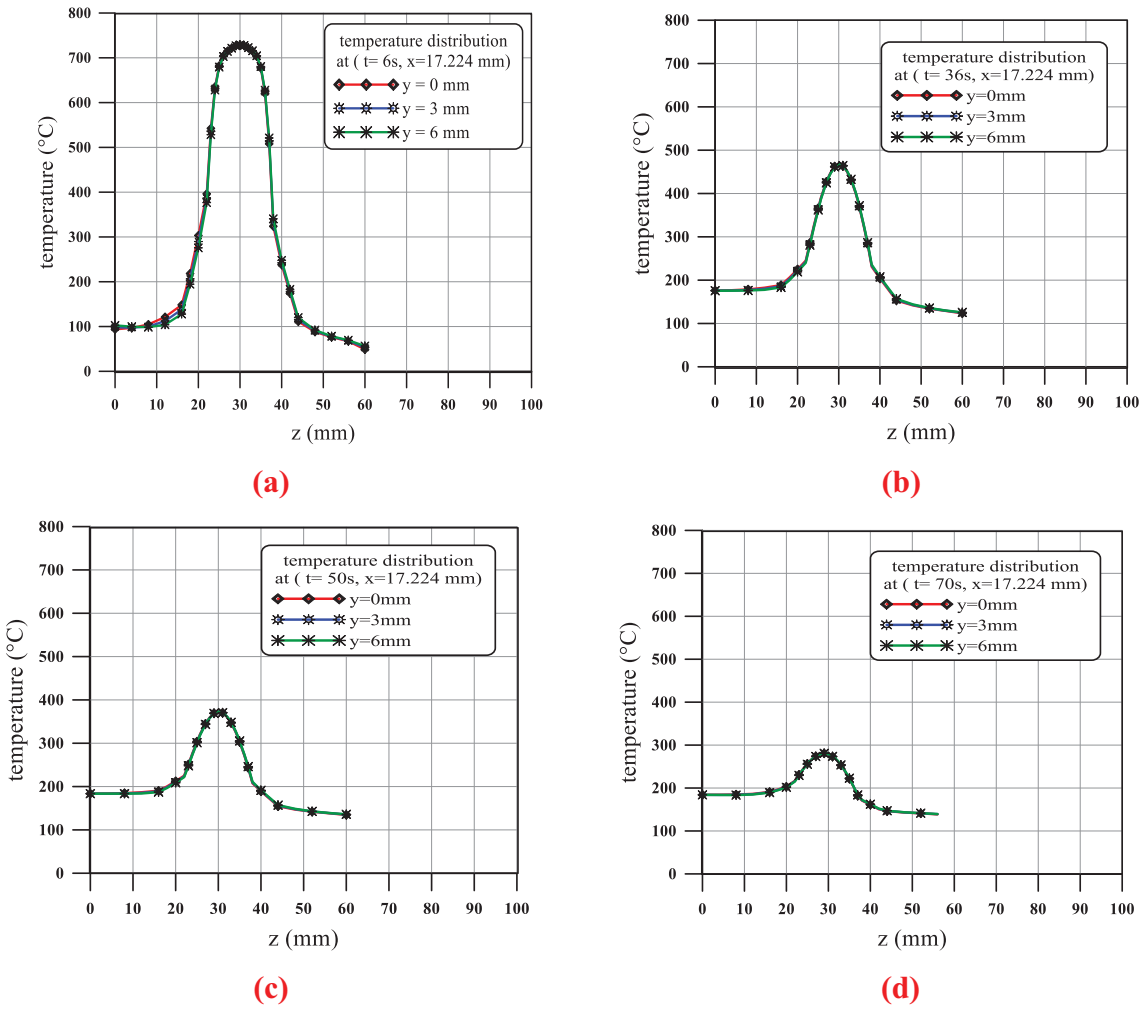

Fig. (7) Computational Temperature Distribution of Experiment (No.19) , a) at Time 6s of the Welding Process, b) at Time 36s of the Welding Process, c) at Time 50s of the Welding Process, d) at Time 70s of the Welding Process

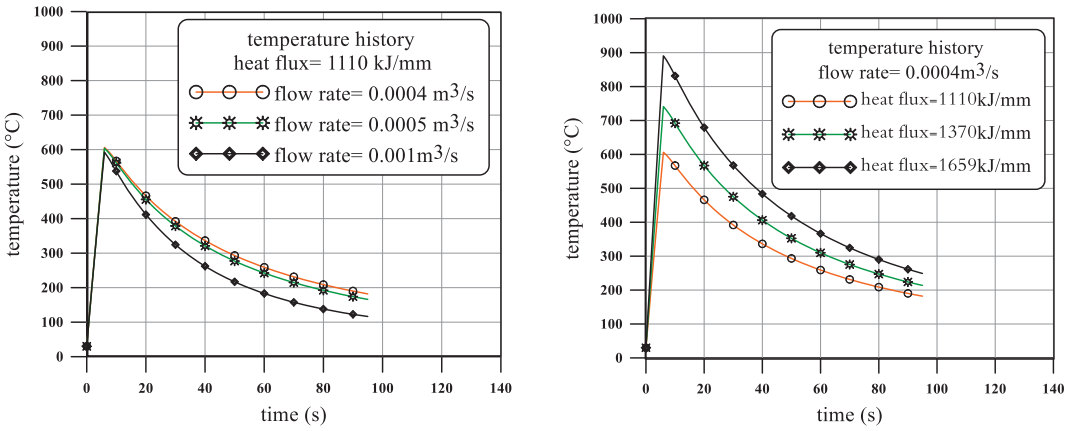

(a) (b)

Fig. (8) Effect of Heat Flux and Flow Rate on the Computational Temperature History, a) Constant Heat Flux, b) Constant Flow Rate

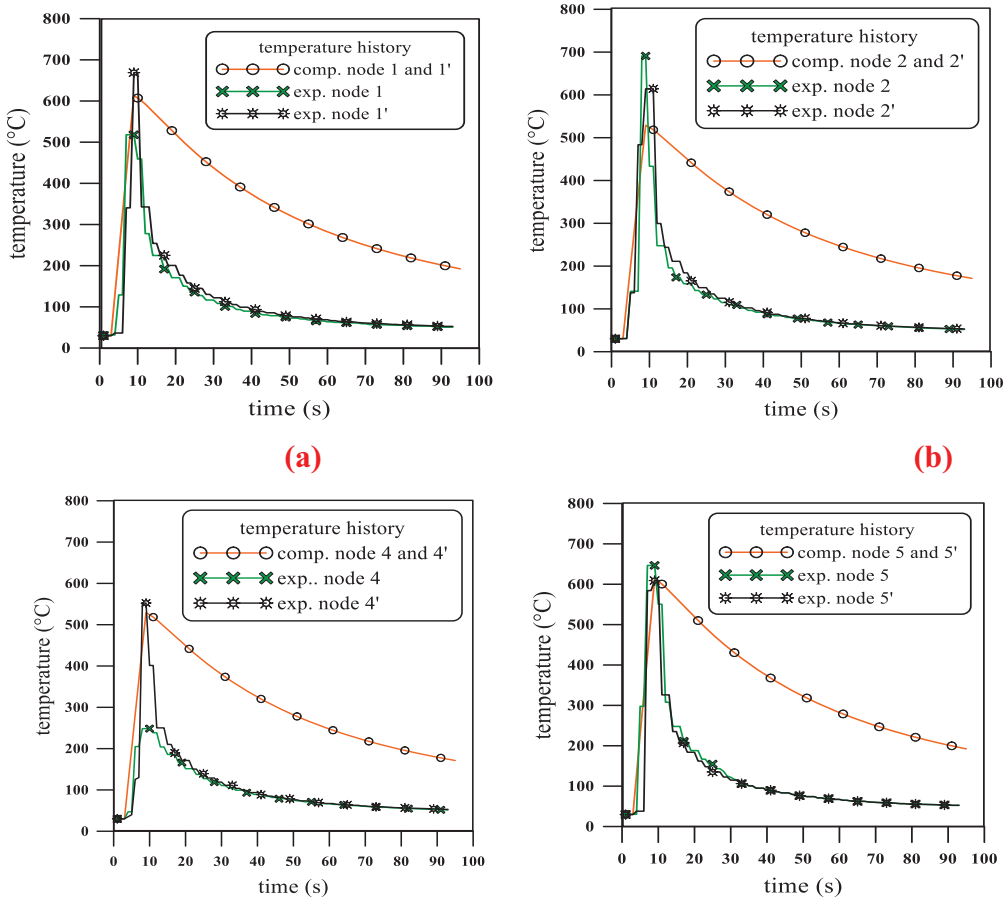

(a) (b)

(c) (d)

Fig. (9) Comparison between Computational and Experimental Temperature History of Experiment (No. 19) , a) 1 and 1', b) 2 and 2', c) 4 and 4', d) 5 and 5'

References:

1. gas pipe", J. of engineering physics and thermodynamic, vol. 83, no. 5, pp. 1028-M.A. Wahab, P.N Sabapathy and M.J. painter, " The onset of pipe wall failure during in-service welding of gas pipeline", J. of material processing technology. 168, pp. 414-442, (2005).
2. P.N. Sabapathy, M.A. Wahab[a,]*, M.J. Painter[b], "The prediction of burn-through during in-service welding of gas pipelines", International journal of pressure vessels and piping, Vol.77, pp.669-677, (2000).
3. P.N. Sabapathy[a], M.A. Wahab[a,]*, M.J. Painter[b], "Numerical models of in-service welding of gas pipelines", J Mater Process Technol 2001; 118:14-21.
4. A.S. Oddy and J.M.J. McDILL, "Burn through prediction in pipeline welding", Int. J. of fracture , Vol. 97، pp. 249-261,(1999).
5. M.A. Wahab, P.N Sabapathy and M.J. painter, "The onset of pipe wall failure during in-service welding of gas pipeline", J. of material processing technology. 168,pp. 414-442, (2005).
6. A.P. Cisilino , M.D. Chapetti and J.L. Oteguï", "Minimum thickness for circumferential sleeve repair fillet welds in corroded gas pipelines", Int. J. of pressure vessels and piping, vol. 79, pp. 67-76, (2002).
7. Rao, S., S., "The Finite Element Method in Engineering", PERGAMON PRESS, (1982).
8. Rozzi,J.C., Pfe€erkorn,F.E., incorpera,F.P., shin, Y.C., "Transient 3-Dimensional Heat Transfer Model for the Laser Assisted Machining of Silicon Nitride: 1. Comparsion of Predictions with Measured Surface Temperature Histories ", Int. J. of Heat and Mass Transfer, 43, (2000), 1409-1424.
9. P.Holman (1997) "Heat transfer" Me GRAW-=Hill.INC. Eighth Edition.
10. Li Chaowen[a,]*, Wang Yong[b], "Three-Dimensional Finite Element Analysis of Temperature and Stress Distribution for in-Service Welding Process", J.material and design.Vol.52, pp.1052-1057, (2013).
11. Tashiro, Taka & Ushio, "Numerical Simulation of Gas Tungsten Arc Welding in Different Gases Atmosphere", J. of Transaction of JWRI, Vol. 34, (2005), pp. 1567-1573.

12. Smith, I., M., and Griffths, D., V., "Programming the Finite Element Method", John Wiley, Inc., (1998).
13. Hamed Masumi Asl and Ali vatani, "numerical analysis of the burn-through at in-service welding of 316 stainless steel pipeline", Int. J. of pressure vessels and piping, Vol. 105-106, pp. 49-59, (2013).
14. Ivan Samardžić, Marko Dunđer, Zvonimir Kolumbić, "Arc Welding of Steel Pipe Connection on Steel Gas Pipeline in-service".
15. J. A.Dantzig, "Modeling Solidification Processes Using FIDAP", Cryst. Res. Technol., 34, (1999).
16. Li Chaowen[a,*], Wang Yong[b], "Three-Dimensional Finite Element Analysis of Temperature and Stress Distribution for in-Service Welding Process", J.material and design.Vol.52, pp.1052-1057, (2013).
17. Mads Martnussen, "Numerical modeling and model reeducation of heat flow in robitic welding", MS.c. Thesis, department of engineering cybernetics, Norwegian University of Science and Technology, (2007).
18. P.N. Sabapathy[a], M.A. Wahab[a,*], M.J. Painter[b], "the prediction of burn-through during in-service welding of gas pipelines", International journal of pressure vessels and piping, Vol.77, pp.669-677, (2000).
19. Tao HAN, Yong WANG and LIU, "study on burn through prediction of in-service welding", J. of transaction of JWRI, pp. 9-12, (2011).
20. V.I. Baikov, I.A. Gishkelyuk, A.M. Rus', T.V. Sidorovich and B.A. Tonkonogov, " Simulation of a manual electric-arc welding in a working gas pipeline/ formulation of the problem", J. of engineering physics and thermodynamic, vol. 83, no. 5, pp. 1016-1027, (2010).
21. V.I. Baikov, I.A. Gishkelyuk, A.M. Rus', T.V. Sidorovich and B.A. Tonkonogov, "Simulation of a manual electric-arc welding in a working gas pipeline/numerical investigation of the temperature-stress distribution in the wall of a1035, (2010).